Chaotic Dynamics with Multiple Iterations of the Chua Circuit

Syed Murtaza Husain
PHY 353L Modern Laboratory
Department of Physics
The University of Texas at Austin
Austin, TX 78712, USA

November 24, 2025

Abstract

In this experiment, we investage chaotic dynamics in two implementations of the Chua circuit: a manually-assembled version and a pre-assembled laboratory circuit. Voltages across the circuit's capacitors were recorded for varying potentiometer values, and the resulting data were analyzed to determine how chaotic each circuit was and to characterize their dynamical properties through several methods. The Feigenbaum constant was estimated twice with data from each circuit, $\delta_{\text{manual}} = 2.74 \pm 0.02$ and $\delta_{\text{pre}} = 4.07 \pm 0.28$, where both were of the correct order of magnitude, with the pre-assembled circuit more closely matching the theoretical value of $\delta \approx 4.669$. Lyapunov exponent fits gave positive exponents of $\lambda_{\text{CH1}} \approx 9.7 \times 10^3$ s^{-1} and $\lambda_{\text{CH2}} \approx 1.3 \times 10^4$ s^{-1}, which confirms that the signals of both circuits evolve chaotically. Bifurcation diagrams show the manually-constructed circuit enter the chaotic regime as $\Omega_1/\Omega_2 \to 1$, while kernel density estimation (KDE) of phase space distributions showed lower density peaks the pre-assembled circuit which is consistent with chaotic behavior. The manually-assembled circuit exhibited semi-chaotic dynamics with some superimposed periodicity.

1 Introduction

1.1 Physics Motivation

In physics, chaos theory is a field of study that is concerned with deterministic dynamical systems that are especially sensitive to changes in initial conditions, and how they behave. Chaotic systems exhibit behavior that appears random even though the underlying physics of all of these systems is well known and the immediate next configurations of a system can be determined from its current state [2]. Meterologist and mathemetician Edward Lorenz is often called the godfather of chaos theory, and his work in the early 1960s in which he studyied simplified numerical models of atmospheric convection were vital to the development of the field. Lorenz took an interest in an experiment in which a cylindrical vessel with water was rotated, and heated and cooled at different points to create 'nonperiodic and unstable' behavior [9]. Lorenz recognized that this behavior that was displayed during turbulent flow in hydrodynamics experiments like these were actually part of something more fundamental about natural processes.

Mitchell Feigenbaum, another physicist who pioneered chaos theory after Lorenz's foundational work, determined that there were certain universal constants and patterns associated with chaotic be-

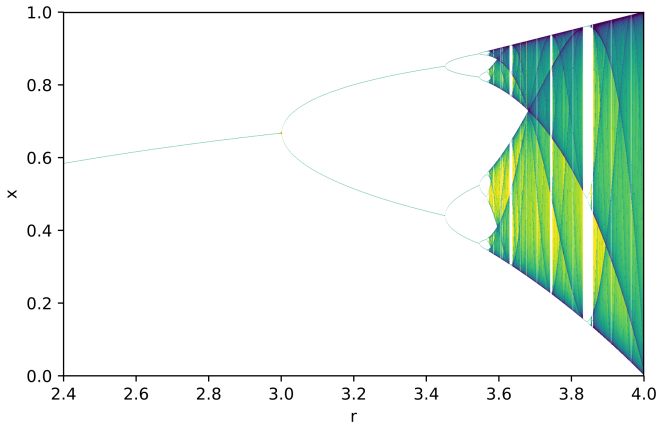

Figure 1: A bifurcation diagram of the logistic map. Values of the population growth parameter r show increasing bifurcations, with highly chaotic behavior being observed at $r \approx 3.6$. Image taken from [11].

havior [10]. When considering chaotic systems that can be described with a single parameter, Feigenbaum determined that the bifurcations, which are changes in the topological structure of the system, which occur are related to these parameters with a constant [7]. This constant has been observed to hold in many different chaotic systems, and is known as the Feigenbaum constant, $\delta \approx 4.6692$ [13].

One of the most famous examples of a chaotic dynamical system is the logistic map, which is a recursive version of the logistic function that can model nonlinear dynamics in populations. It is defined as

$$x_{n+1} = r x_n (1 - x_n) \tag{1}$$

where $0 < x_n < 1$ is a population parameter, and r is a constant that represents the rate of growth of the population [12]. With r as a parameter to be varied, the logistic map provides interesting behavior in which it is easy to observe that certain values of r provide more deterministic values for population, while higher values cause oscillatory or wildly chaotic behavior. A visualization of the logistic map is shown in figure

Studying chaotic dynamics is an important and highly interesting topic in physics, with many reseracherrs believing that the universality of bifurcation theory and the Feigenbaum constant are far deeper than previously believed [18].

1.2 Lorenz Attractor

Lorenz created an atmospheric convection model in 1963 which gives rise to an interesting chaotic shape known as the Lorenz attractor. The model he created is as follows:

$$\frac{dx}{dt} = \sigma(y - x) \tag{2}$$

$$\frac{dy}{dt} = x(\rho - z) - y \tag{3}$$

$$\frac{dz}{dt} = xy - \beta z \tag{4}$$

where x, y, z are phase space variables of the system, and σ, ρ, β are parameters for each part of the system like the Prandtl number or Rayleigh number

For specific parameter values, the plot of the solution becomes a chaotic oscillating shape with infinite perimeter but finite area, an attractor. This attractor has deterministic evolution, non-periodic trajectories, and fractal geometry which are all hallmarks of a chaotic system.

1.3 The Chua Circuit

Leon Chua invented the now famous Chua circuit in 1983. This circuit is unique because it is a very simple setup in which it is possible to observe chaos, producing a Lorenz attractor and allowing physicists to study chaotic behavior in-depth [16].

Chua's original circuit has two capacitors and an inductor to store energy, as well as a Chua diode, a chaotic oscillating circuit element. Chua diodes can be constructed from op-amps, as we will show later.

If the voltage across the capacitors are C_1 and C_2 and the inductance is L, then the circuit is described

by this set of differential equations:

$$\frac{dv_1}{dt} = \frac{1}{C_1}\left(G(v_2 - v_1) - g(v_1)\right), \tag{5}$$

$$\frac{dv_2}{dt} = \frac{1}{C_2}\left(G(v_1 - v_2) + i_L\right), \tag{6}$$

$$\frac{di_L}{dt} = \frac{1}{L}\left(-v_2 - R_0 i_L\right), \tag{7}$$

$$g(v_R) = \begin{cases} G_b v_R + (G_b - G_a)E_1, & \text{if } v_R \le -E_1, \\ G_a v_R, & \text{if } |v_R| < E_1, \\ G_b v_R + (G_a - G_b)E_1, & \text{if } v_R \ge E_1. \end{cases}$$

where $g(v_1)$ is a function that accounts for the Chua diode behavior, and v_1, v_2 are voltages across each capacitor [1]. Values for resistors in Chua's circuit act as the varying parametrs for the chaotic system.

1.4 Feigenbaum Constant

The Feigenbaum constant, δ, as discussed in the previous section, represents the spacing between bifurcations when a parameter is varied in a chaotic system like the logistic map or Chua circuit [10].

The Feigenbaum constant is defined as:

$$\delta = \lim_{n\to\infty} \frac{a_n - a_{n-1}}{a_{n+1} - a_n}$$

where a_n is the value for the varied parameter (such as resistance) at which the n-th bifurcation happens, or in other words, when the period doubles [10] [18].

To calculate the Feigenbaum constant in a chaotic system, the only data that is needed is then information about period doublings and the parameter values at which they take place.

1.5 Bifurcation Diagrams

Bifurcation diagrams are visualizations that show how bifurcations occur with parameter varying. An example for the logistic map is shown in figure 1. These diagrams are made by sweeping the parameter and taking measurements of period values of the system [3] [5].

Most bifurcation diagrams have a clear cut-off point that shows where chaotic behavior truly emerges, and in the example shown in fig 1, this point can be seen at $r \approx 3.6$. At this point, the system starts exhibiting extremely complex dynamics that can not be easily predicted [12].

1.6 Lyapunov Exponent

Lyapunov exponents are useful in chaotic dynamics to understand how sensitive the system is to initial perturbations [17]. They measure the average exponential rate when phase space trajectories diverge or converge over time. To calculate the Lyapnuov exponent, we can use the following formula

$$\lim_{n\to\infty} \frac{1}{t}\sum_{i=0}^{t-1} \log|\frac{dF}{dx}|_{x=x_i}| \tag{8}$$

where the function $F(x)$ represents the state of the system at a parameter value, and t is time [17].

1.7 Power Spectra

Taking a power spectum of a chaotic system's behavior across individual experimental runs can be a useful way to find out if there is underlying periodicity in the data. For a truly chaotic system, the spectrum should be filled with noise and have very weak peaks, because otherwise the system actually has significant periodicity and is not fully chaotic [19].

We can use the Fast Fourier Transform (FFT) to get spectral components of chaotic system data:

$$P(f) = |\mathcal{F}\{x(t)\}|^2$$

where $\mathcal{F}\{x(t)\}$ is the Fourier transform of the system's time domain values $x(t)$, and $P(f)$ is the power at frequency f [20].

1.8 Kernel Density Estimation

A useful way to analyze the probability density of a chaotic system's states is to use Kernel Density Estimation (KDE). This technique can be applied to a chaotic system to discover which regions are more likely for the system to settle into, and can help determine how chaotic a system is or how much periodicity it contains, similar to the power spectrum [6].

Finding the KDE for a set of n data points $\{x_i\}_{i=1}^{n}$ can be done with:

$$\hat{f}_h(x) = \frac{1}{nh} \sum_{i=1}^{n} K\left(\frac{x - x_i}{h}\right)$$

where K is the kernel function, and h is the bandwidth parameter. When h is smaller, we obtain a more sensitive estimate, and a larger h gives a smoother density [8].

1.9 Equipment Background

The equipment for this experiment involved several electronic components, as well as breadboards and jumper wires to connect them, and oscilloscopes and miultimeters to take measurements. In particular, the TL082 operational amplifier (op-amp) was instrumental to simulate an inductor and Chua diode in our circuit.

The TL082 is a JFET op-amp that has a dual configuration, meaning the circuit can be constructed more cleanly using two TL082s rather than 4 regular single package op-amps. Each TL082 must be given rail voltages of $\pm 15\ V$ and each side of the IC has inverting inputs, noninverting inputs, and outputs [15].

The digital oscilloscope utilized in this experiment is also of key importance. We use a Tektronix TBS 1062 two-channel oscilloscope which is used to read the voltage of both capacitors in the circuit, and save their individual waveforms on a USB flash drive which can then be analyzed against each other [14].

1.10 Our Approach

We construct a Chua circuit using TL082 op-amps and potentiometers, and take several readings, varying the values Ω_1, Ω_2 of the potentiometers. Using this circuit and data collected from the laboratory's example Chua circuit which generates a perfect Lorenz attractor. From this data, we construct a bifurcation diagram, try to estimate Feigenbaum's constant, create KDE plot and find the largest Lyapunov exponent for different trials, and determine the power spectra of the circuits.

2 Experimental Setup

2.1 Apparatus

We construct a version of the Chua circuit shown in figure 2. This Chua circuit utilizes TL082s to simulate the inductor and Chua diode of the original circuit. The left portion (inductor) utilizes the nonlinear feedback characteristic of the op-amps to create a biased output line between U_2 and the capactior, which causes unstable oscillations. To the right, the nonlinear ramping of a Chua diode is simulated by using difference resistor values and tying both sides of the TL082 together [1].

2.2 Data Collection

Three distinct phases of data collection were carried out. The first of these was done by varying the values of Ω_1, Ω_2 and measuring them using the multimeter for our constructed circuit 2 and recording the voltages across capacitors C_2, C_3 using the oscilloscope's read out feature. The list of these readings is shown in figure 1, and several runs are shown in figure 4.

Next, we take similar readings from the lab's example Chua circuit, which has been pre-constructed and displayed a Lorenz attractor immediately upon measurement. This data is displayed in table 2 and some characteristic runs are shown in figure 3. We note that there is a lack of data due to time con-

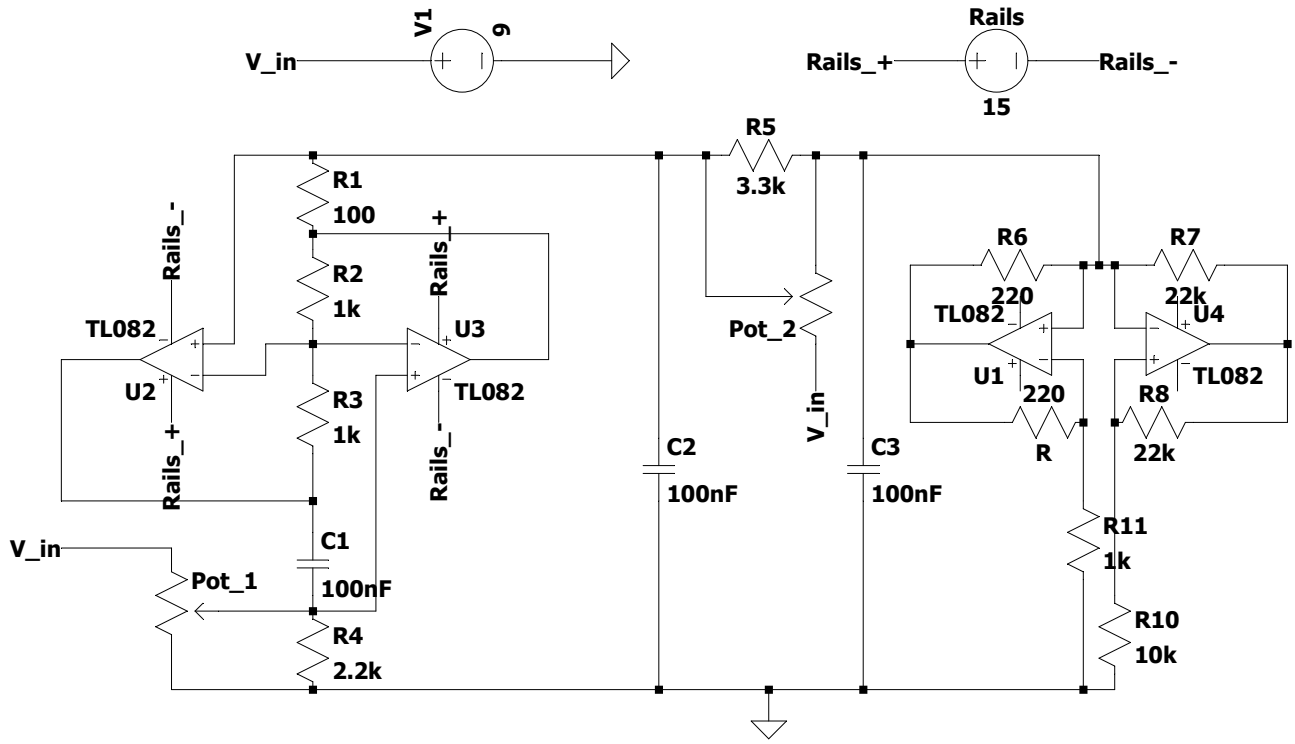

Figure 2: A version of the Chua circuit detailed in [1]. Chaotic behavior is observed for certain values of the potentiometers Pot 1 and Pot 2, at which bifurcations take place and the xy graph folds over itself.

straints in the lab, and more data varying both resistance parameters would be ideal.

Finally, returning to the circuit we manually assemble, we take readings swapping V_in for a function generator and vary voltage amplitude, frequency, and pulse shape to obtain very interesting phase portraits displayed in section 4.5.

2.3 Measurement Error Analysis

The Tektronix oscilloscope has a finite voltage measurement resolution and sample rate. Each channel readinghas an approximate uncertainty of

$$\sigma_V \approx \pm(0.01 \times V_{\text{reading}} + 2 \text{ mV}),$$

which propagates into all calculations [14]. Meanwhile, our digital multimeter's measurement error comes from the least count precision in resistance measurements. Precisions for each specific measurement are shown in tables 1 and 2.

In bifurcation spacing calculations, the uncertainty in resistance propagates as [4]:

$$\sigma_\delta = \delta\sqrt{\left(\frac{\sigma_{\Omega_1}}{\Omega_1 - \Omega_0}\right)^2 + \left(\frac{\sigma_{\Omega_2}}{\Omega_2 - \Omega_1}\right)^2}$$

For calculations that require oscilloscope and resistance data, the error propagation is:

$$\sigma_f = f\sqrt{\left(\frac{\sigma_V}{V}\right)^2 + \left(\frac{\sigma_t}{t}\right)^2}, \quad \sigma_\lambda \approx \left|\frac{d\lambda}{dV}\right|\sigma_V + \left|\frac{d\lambda}{d\Omega}\right|\sigma_\Omega$$

Run #	Ω_1 **(R1),** $\pm 0.005\Omega$	Ω_2 **(R2)**	**Bifurcation Notes**
10	$488\,\Omega$	$1.576\,\text{k}\Omega \pm .5\Omega$	Yes
11	$468\,\Omega$	$1.575\,\text{k}\Omega \pm .5\Omega$	Yes
12	$467.8\,\Omega$	$1.767\,\text{k}\Omega \pm .5\Omega$	Yes
13	$417.2\,\Omega$	$1.767\,\text{k}\Omega \pm .5\Omega$	Yes
14	$366.4\,\Omega$	$1.82\,\text{k}\Omega \pm .5\Omega$	No (min Ω_1)
15	$306\,\Omega$	$1.55\,\text{k}\Omega \pm .5\Omega$	Somewhat bifurcating (min Ω_2)
16	$597.2\,\Omega$	$1.55\,\text{k}\Omega \pm .5\Omega$	Somewhat bifurcating (max Ω_1)
17	$572\,\Omega$	$1.94\,\text{k}\Omega \pm .5\Omega$	Many points
18	$585\,\Omega$	$0.4\,\Omega \pm .05\Omega$	Many points
19	$578\,\Omega$	$0.5\,\Omega \pm .05\Omega$	Many points (min Ω_2)
20	$594\,\Omega$	$835\,\Omega \pm .5\Omega$	Repeating pattern
22	$590\,\Omega$	$591\,\Omega \pm .5\Omega$	Too noisy, $\Omega_1 = \Omega_2$

Table 1: Potentiometer values and qualitative bifurcation observations for each run of the assembled Chua circuit. The sweep parameter was Ω_1 as well as the ratio of potentiometer values.

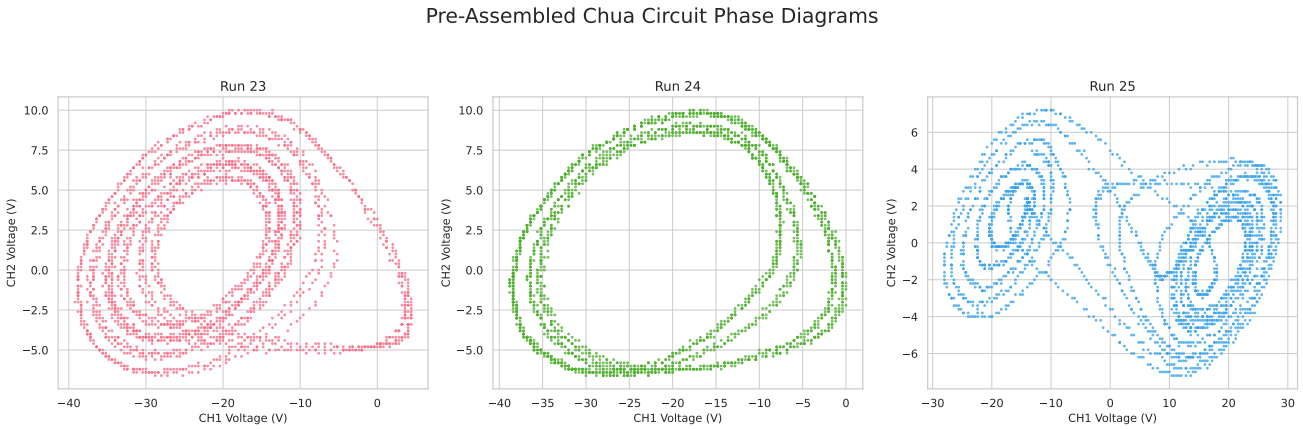

Figure 3: Data collected from the pre-assembled modern lab Chua circuit, which displayed Lorenz attractor behavior. Resistor values for each displayed run is shown in table 2. Attractor behavior can be seen to change for different ratios of Ω_1, Ω_2, with larger Ω_1 splitting the butterfly-like pattern into just halves.

Run #	Ω_1 **(R1),** $\pm 0.5\Omega$	Ω_2 **(R2),** $\pm 5\Omega$
23	$872\,\Omega$	$1.80\,\text{k}\Omega$
24	$834\,\Omega$	$1.80\,\text{k}\Omega$
25	$774\,\Omega$	$1.80\,\text{k}\Omega$
26	$876\,\Omega$	$1.66\,\text{k}\Omega$
27	$857\,\Omega$	$1.49\,\text{k}\Omega$

Table 2: Potentiometer values for each run of the pre-assembled Chua circuit. The pre-assmebled lab circuit displayed clean Lorenz attractor behavior and less data was taken due to time constraints. For extreme resistance values, the attractor behavior was weaker.

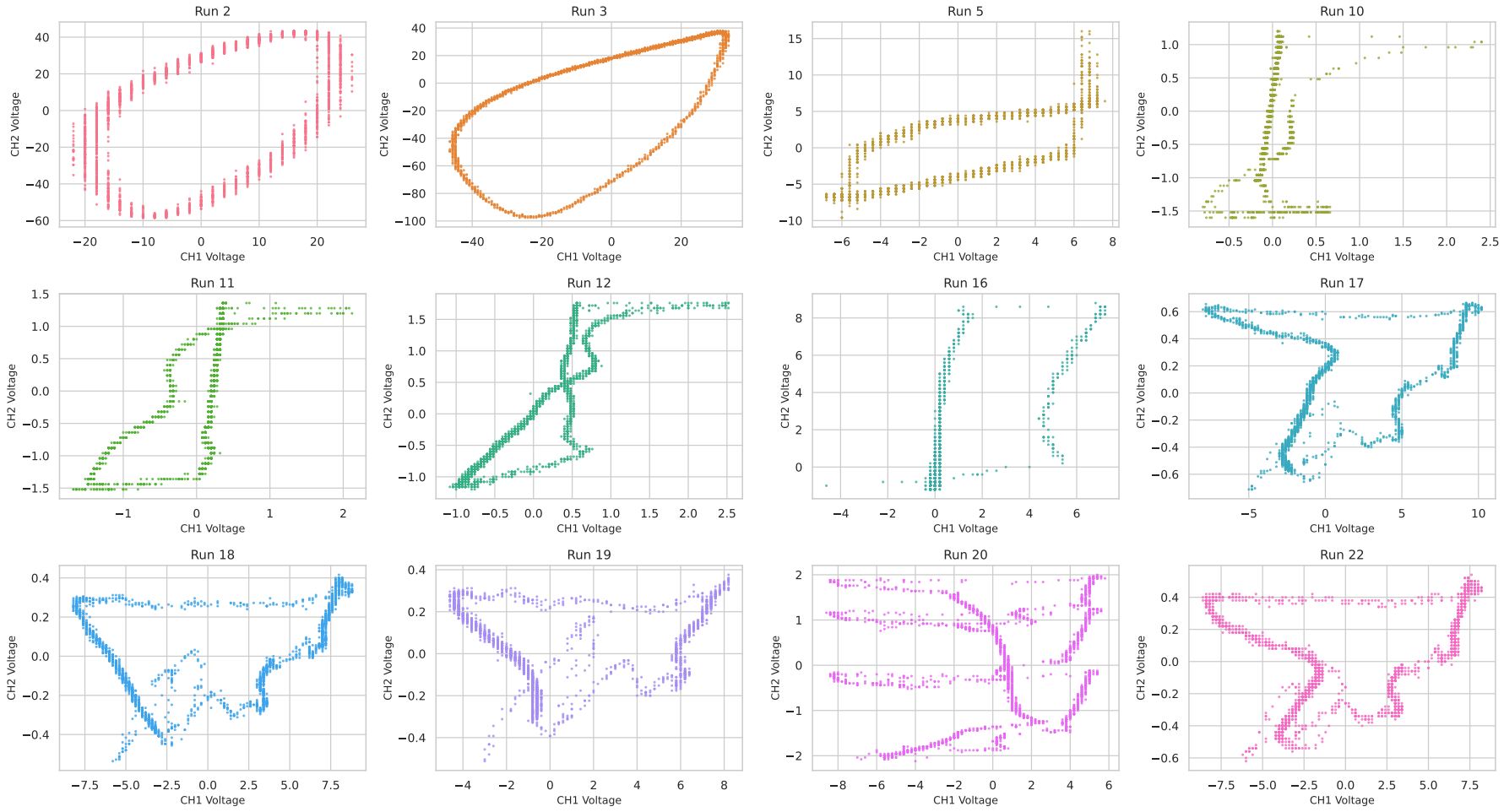

Figure 4: 12 experimental trials for manually-constructed Chua circuit, shown in figure 2. Some attractor-like behavior can be seen within run 20 and others show circular phase space portraits which align with some behavior regimes of the standard Chua circuit. Overall, no Lorenz attractor is observed, but some chaotic behavior is undoubtedly

3 Data Analysis and Results

3.1 Estimating Feigenbaum's Constant

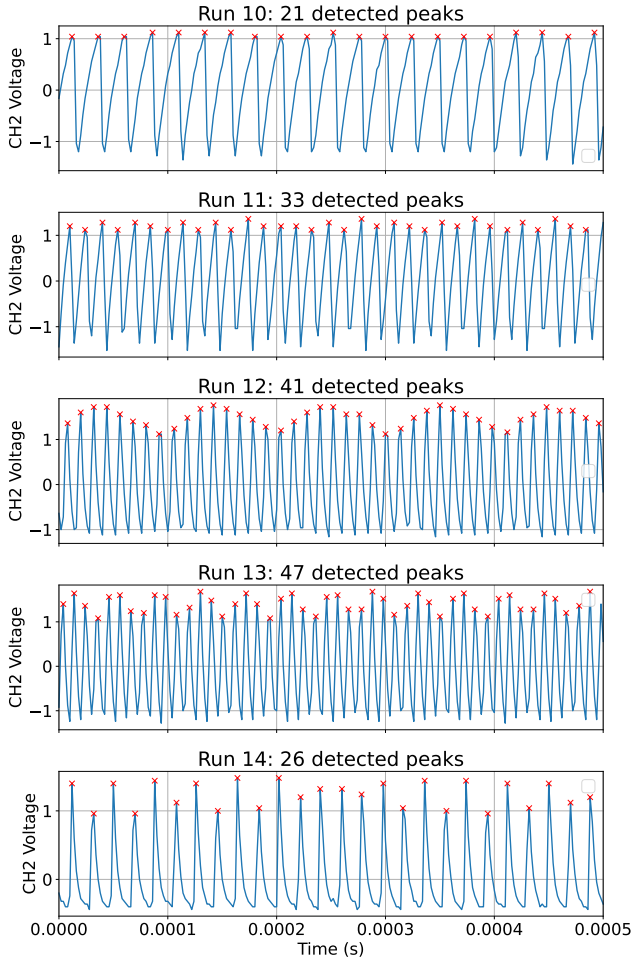

Figure 5: Periodicity for different values of the potentiometers, Ω_1, Ω_2 for the implementation of the Chua circuit shown in figure 2. The frequencies of different runs can be used to estimate the Feigenbaum constant. Values of Ω_1, Ω_2 are shown in table 1.

Using the data gathered across both circuits, shown in tables 1 and 2, we can obtain an estimate for the Feigenbaum constant using the theory outline in section 1.4. First, we must determine the periodicity of each oscilloscope channel of each run to determine when bifurcations happen within the circuit. Examples of this periodicity determination are shown in figure 5. For this calculation, we use the varied parameter a_n to be Ω_1/Ω_2 and the bifurcation points to be our detected peaks. Then finally, we obtain estimates of the Feigenbaum constant for both the manually-assembled and pre assembled lab circuits:

$$\text{Manual Circuit: } \delta = 2.74 \pm .0208 \tag{9}$$

$$\text{Pre-assembled Circuit: } \delta = 4.07 \pm .282 \tag{10}$$

3.2 Lyapunov Fit

The largest Lyapunov exponent (LLE) fits are calculated using the theory in section 1.6 across several different experimental runs are shown in figure 6. Each curve is the logarithm of trajectory and the LLE is gotten through a slope fit.

Calculations for 11, 12, and 16 (pictured in figure 4) are shown in figure 6. These three runs are from the manually assembled Chua circuit, while run 23 (picutred in figure 3) is taken from the pre-assmebled circuit with a correct Lorenz attractor.

Run 23's calculation shows no clear oscillatory pattern and instead, the divergence increases with time in an expected manner. However, the other three runs show clear periodicity at the beginning with the divergence smoothing out still retaining some overall periodicity. This interesting result shows that the other three runs are semi-chaotic, as they show periodic behavior that is overlayed on the underlying chaotic behavior. This suggests that the manually assembled circuit has errors which cause leakage of periodicity into the circuit's signal.

The extracted largest Lyapunov exponents for the fully chaotic run were

$$\lambda_{\text{CH1}} \approx 9.7 \times 10^3 \pm 30 \text{ s}^{-1} \quad \lambda_{\text{CH2}} \approx 1.3 \times 10^4 \pm 30 \text{ s}^{-1}$$

which are both positive and of the same order of magnitude, which is what we expect for deterministic chaos. The earlier runs also have a positive $\lambda_{\max}$

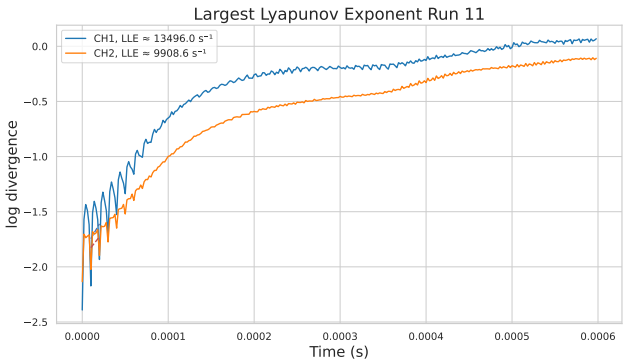

(a) Run 11

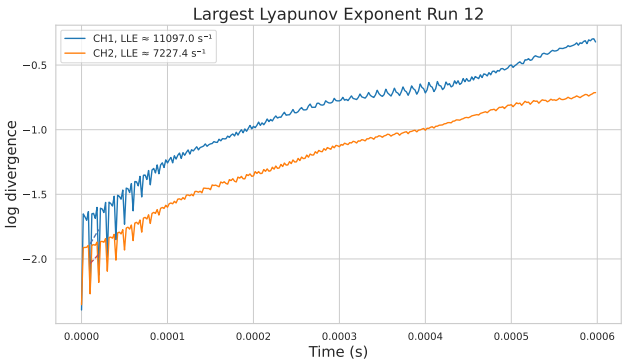

(b) Run 12

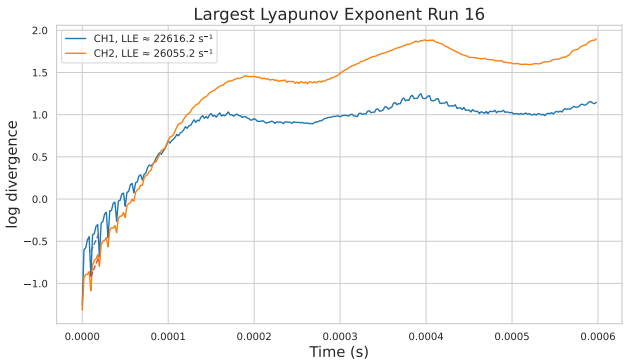

(c) Run 16

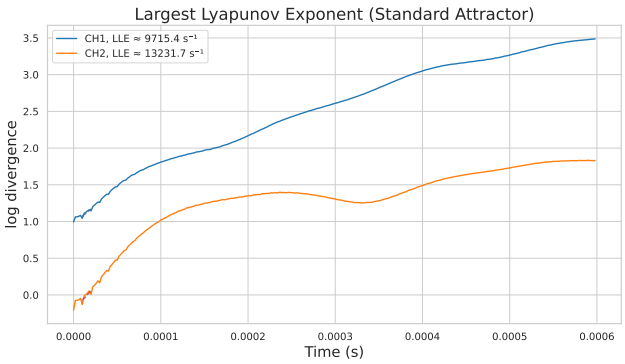

(d) Lorenz Attractor (Run 23)

Figure 6: Largest Lyapunov Exponents (LLEs) calculated for several experimental runs, with runs 11, 12, and 16 being conducted on the manually-construced circuit, and run 23 being conducted on the pre-constructed lab circuit. The pre-constructed circuit has extremely slight periodicity at the beginning which is smoothed out over time, while other runs have clearly continuing periodicity, suggesting that they are not fully chaotic.

values but the clear periodicity means that their behavior is not fully chaotic, but instead falls into a chaotic regime given some time to smooth out their oscillatory behavior.

3.3 Bifurcation Diagram

To construct bifurcation diagrams for the manually-constructed Chua circuit, we isolate each run and plot each data point according to peak wave voltage against the control parameter Ω_1/Ω_2. Figure 7 shows the bifurcation diagram shifted by the relative phase of the peak. Each point is phase shifted only to make the bifurcation diagram visually clearer. Meanwhile, the diagram shown in figure 9 shows each set of points from each run at the parameter value, and has spline fits between each cluster of points. Points were clustered using the same KDE function discussed in secitno 1.8.

This bifurcation diagrams agree with the results of the previous LLE calculation, as there are clear strong period separations for each run, with there being intermediary points which represent the chaotic behavior interspered with chaotic behavior. Certain values of the parameter are also more chaotic than others, with runs 16 and 20 (gold and grey in fig 7) spreads being less clearly separated by period.

3.4 Power Spectrum

Using the theory outlined in section 1.7, we can take power spectra of individual runs and examine whether or not there is clear periodicity. Power spectra for several experimental runs are shown in figure 8. Runs 11, 12, and 16, which were taken from the manually-assembled Chua circuit, show clear periodicity at harmonic intervals. Meanwhile, run 23, which was conducted on the pre-assmbled lab circuit, has no significant peaks, with noise causing a peak at 0 frequency, a clear sign that there are no periodic signals within the output.

3.5 Kernel Density Plot

The Kernal Density Estimate (KDE) contour plots of different experimental runs can be computed using the process discussed in section 1.8. These plots can be seen in figure 10. Probability densities for run 12, the manually-constructed Chua circuit experimental run, can be seen to peak at a particular point at about $V_1, V_2 = -1$. This peak region contains a probability density of 3.708, while the relative peak of the KDE plot for run 23, taken from the pre-assembled circuit, is only 0.004791. Chaotic systems tend to have more unpredictable configurations, which is directly shown in this KDE plot in which the probability density of the Lorenz attractor exhibiting circuit is much lower than that of run 12, which has been previously seen to exhibit some combination of chaotic and periodic behavior.

4 Summary and Conclusions

4.1 Feigenbaum Constant Analysis

The Feigenbaum constants we calculated,

$$\delta_{\text{manual}} = 2.74 \pm 0.02, \quad \delta_{\text{pre}} = 4.07 \pm 0.282,$$

disagree with the known value but are both within the expected order of magnitude of the theoretical value $\delta \approx 4.669$. The calculation for the pre-assembled circuit is very close but is not within experimental uncertainty, likely due to a lack of data with varying resistance parameters. Meanwhile, the error for the manually constructed circuit is far smaller but does not align with the known value, which is expected after observing many pieces of evidence that the manually constructed circuit is only semi-chaotic.

4.2 Lyapunov Constant Analysis

The Lyapnuov fits for Runs 11, 12, and 16 (from the manual circuit) show clear periodicity before

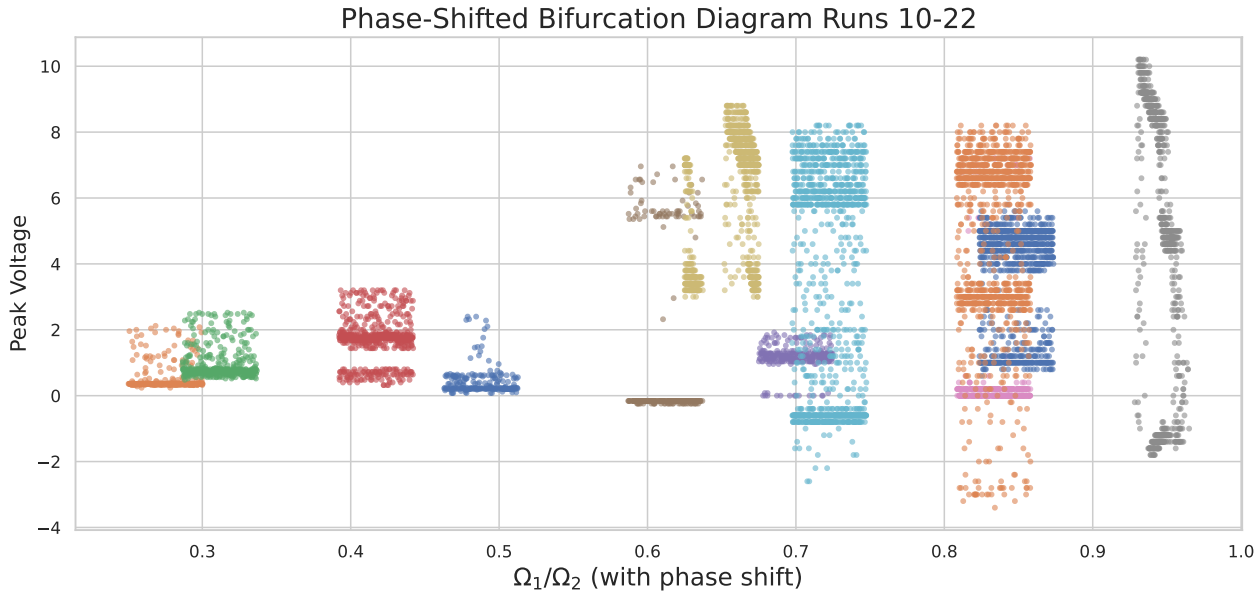

Figure 7: Bifurcation diagram of manually-constructed Chua circuit. Periodicity shows splits between peak voltages that grows with the control parameter, Ω_1/Ω_2, expected for a bifurcation diagram. Each point is shifted left or right using relative phase to make the distribution clearer.

they diverge, which indicates that they are only smi-chaotic. The divergence rate is still positive, but is much smaller in magnitude than that of the fully chaotic Lorenz attractor, shown in Run 23. The pre-assembled circuit shows a smoother increase in log(divergence), more evidence that it is fully chaotic. The measured largest Lyapunov exponents,

$$\lambda_{\text{CH1}} \approx 9.7 \times 10^3 \text{ s}^{-1}, \quad \lambda_{\text{CH2}} \approx 1.3 \times 10^4 \text{ s}^{-1},$$

are both positive and are in the same order of magnitude. This confirms that chaotic behavior is observed in both circuits, with the pre-assembled circuit being much closer to purely chaotic than the manually-assembled circuit.

4.3 Spectrum, Density, and Bifurcation Analysis

The phase-shifted and connected bifurcation diagrams shown in figures 7 and 9 clearly show that the manually-constructed circuit falls into a chaotic regime with period doublings taking place at values for whivh $\Omega_1/\Omega_2 \to 1$. Unfortunately, due to time constraints, there was insufficient data to construct a bifurcation diagram for the pre-assembled circuit.

The power spectra shown in figure 8 and the KDE maps shown in figure 10 both confirm that the pre-assembled circuit displays chaotic behavior while the manually-assembled circuit has some underlying periodicity. In the case of the power spectra, clear peaks can be seen at different harmonics for the manually assembled circuit, which differ with different values of Ω_1/Ω_2. Meanwhile, the standard Lorenz attractor has a peak at 0 Hz, a clear indicator that the signal is dominated by noise and there is no actual periodicity. The KDE plots show that the probability densities of values for phase space locations in the plots of either circuit are orders of magnitude apart. The highest probability region for a run of the manually-constructed circuit is 3.708 while for the pre-assembled circuit, it is 0.004791. This shows that the probabilities are spread very evenly in the chaotic regime while they are more concentrated in the semi-chaotic regime, confirming our intuition.

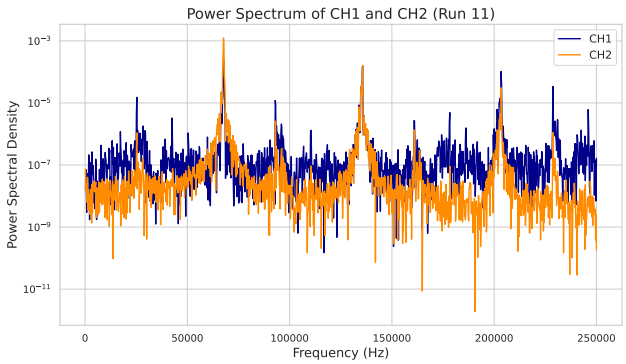

(a) Run 11

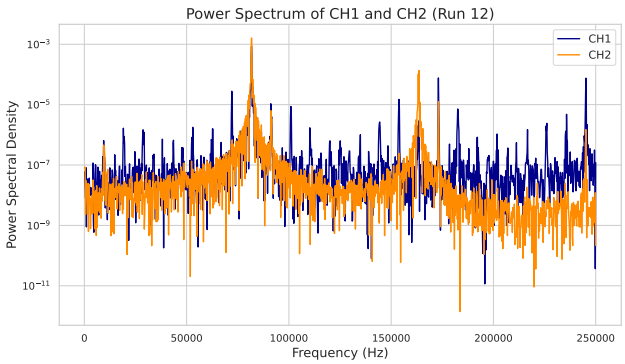

(b) Run 12

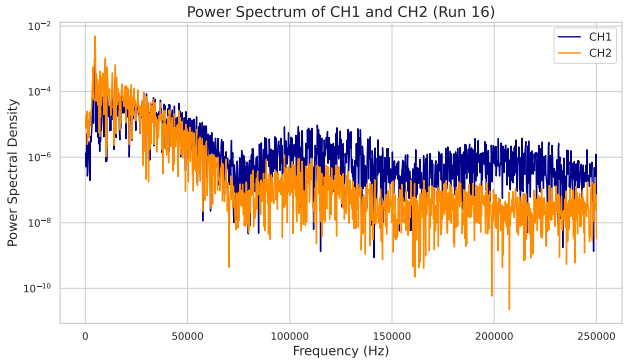

(c) Run 16

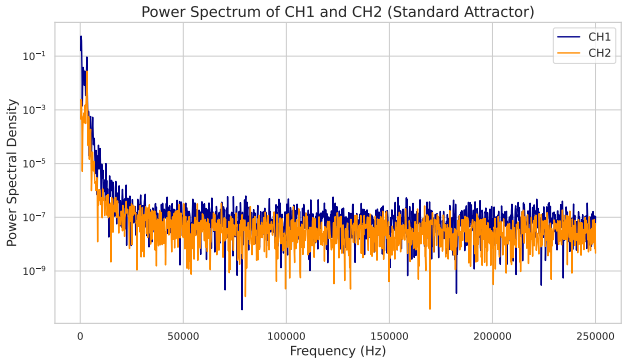

(d) Lorenz Attractor (Run 25)

Figure 8: Power spectra for several different experimental runs of the Chua circuit. Runs 11, 12 and 16 are conducted on the manually-constructed circuit, and run 23 is conducted on the pre-constructed circuit which displayed a clear Lorenz attractor. Clear harmonic peaks can be seen in runs 11 and 12, with run 16 being only slightly more chaotic, whereas run 23 has the expected behavior.

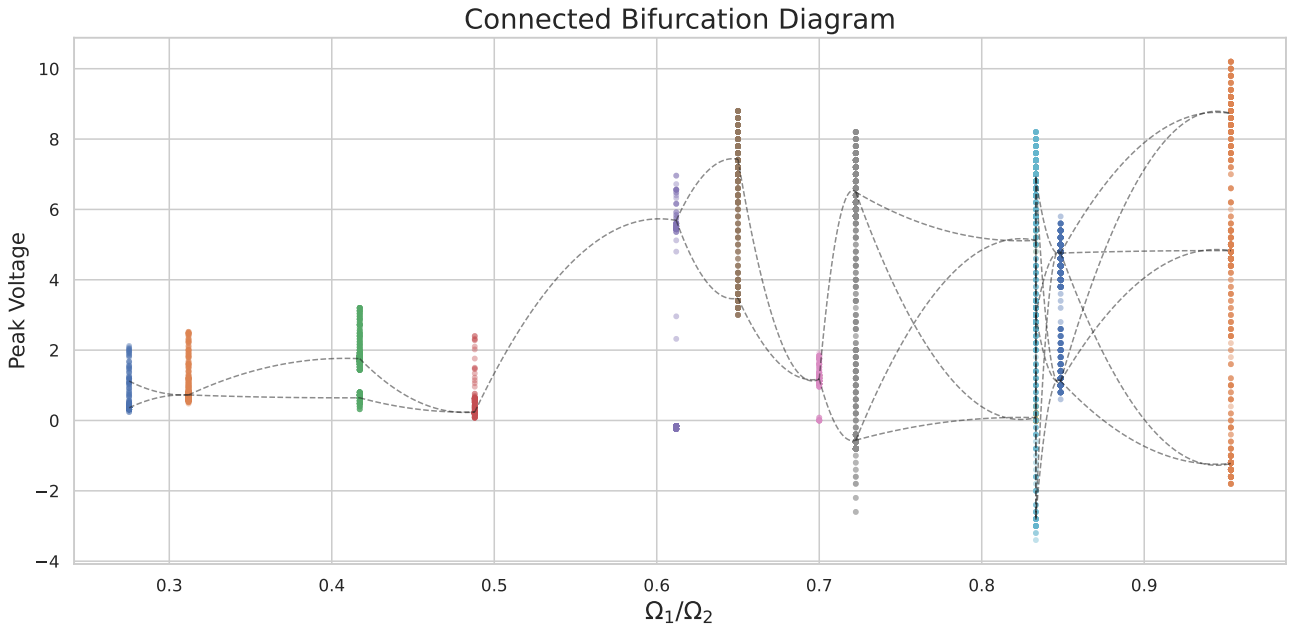

Figure 9: Bifurcation diagram of manually-constructed Chua circuit, with cluster centers connected through spline fits to show perioidicty splits with increasing Ω_1/Ω_2. More periodicity clusters are created as the parameter increasing, implying chaotic behavior.

4.4 Conclusion

In this experiment, we studied two constructions of a Chua circuit, one which generated a standard Lorenz attractor, and another which displayed interesting semi-chaotic behavior. Through several experimental runs, we measured voltages across two capacitors, v_1 and v_2, using a digital oscilloscope, as well as potentiometer resistance values, Ω_1, Ω_2 using a multimeter. After data collection, we utilize several different methods of quantifying the chaotic behavior of each circuit, including determining the largest Lyapunov exponents for different experimental runs, estimating the Feigenbaum constant, creating bifurcation diagrams, examining the power spectra of the circuit output, as well as quantifying the probability density of each circuit's phase space using kernel density estimation.

We estimate the Feigenbaum constant to be $\delta_{manual} = 2.74 \pm 0.02, \delta_{pre} = 4.07 \pm 0.282$, showing a deviation from the known value of $\delta \approx 4.669$, but with the pre-assembled circuit being closer than the manually-constructed circuit.

The largest Lyapunov exponents show divergence growing with $\lambda_{\text{CH1}} \approx 9.7 \times 10^3$ s$^{-1}, \lambda_{\text{CH2}} \approx 1.3 \times 10^4$ s^{-1} for the Lorenz attractor show a smooth increase in divergence as time goes forward, and are of the correct order of magnitude. The LLEs for manually-constructed circuit runs show clear periodicity while still increasing in divergence with time, showing that the circuit exhibits chaotic behavior with periodicity imposed on top of it.

Bifurcation diagrams were created for the manually-constructed circuit, showing a clear increase in periodicity divergence as Ω_1/Ω_2 approaches 1.

Kernel density estimation plots confirm this intuition by showing low relative likelihood areas for the Lorenz attractor at 0.004791, while probabilities are more concentrated for the manually-constructed runs, with run 12 having a highest probability of 3.708. Power spectrum analysis confirms these conclusions by showing no clear periodicity in the spectra of the Lorenz attractor, and slight periodic

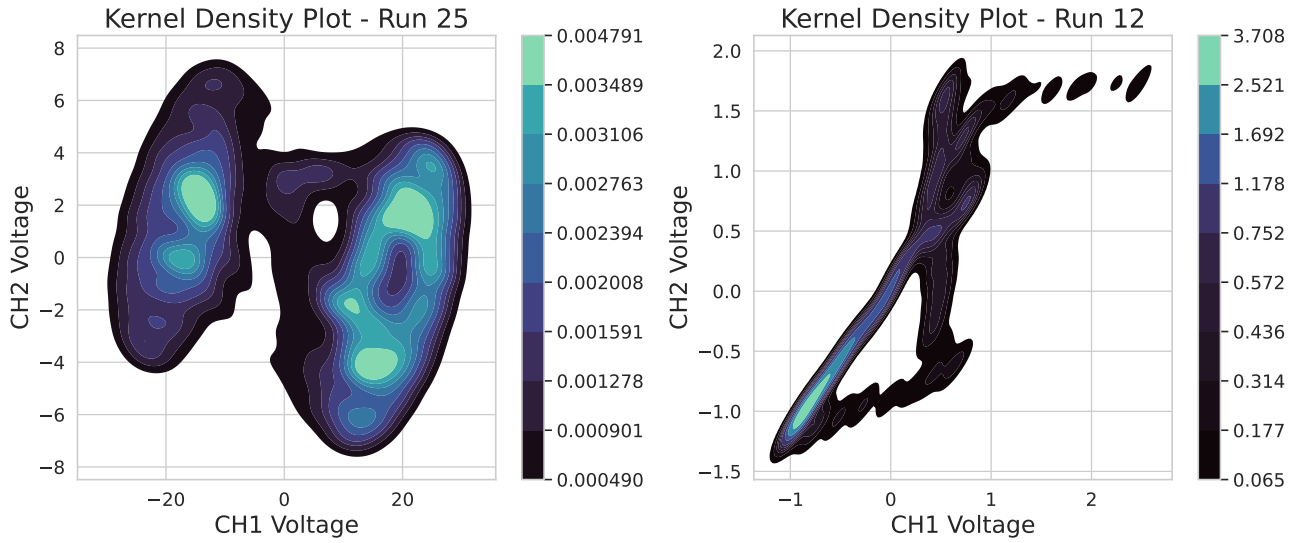

Figure 10: Kernel Density Estimate (KDE) countour maps for two experimental runs of the Chua circuit. Run 23 (left) was collected from the pre-assembled laboratory circuit, and run 12 (right) was collected from the manually-assembled circuit implementation.

signals among the chaotic noise of the manually-constructed circuit.

Overall, we have studied two interesting systems, one fully chaotic and the other semi-chaotic, and have used several techniques to differentiate them and study their properties. In terms of bigger picture physics, studying semi-chaotic and chaotic systems gives us deeper insight into dynamical systems that are vital to understand such as weather systems, and show how complex and unpredictable behaviors can still be studied and quantified. This experiment has been a valuable exercise in the study of chaotic dynamical systems and independent laboratory procedure.

4.5 Very Chaotic Dynamics

As an additional experiment, we utilize a function generator to run different signals in place of V_{in} to the manually-constructed circuit and observe various interesting waveforms. The output of this is shown in figure 17. Several interesting attractor-like shapes can be observed, especially in figure 13, which is similar in shape to a Lorenz attractor, but has much more noise than the shape seen in the pre-assembled circuit output. Some other strange attractor shapes are seen in figures 12 and 15, with repeating patterns that continue downward instead of spiralling inward like the Lorenz attractor.

4.6 Future Work Considerations

Future work might consider taking much more data on a circuit that shows a Lorenz attractor, including a fine sweep of Ω_1 and Ω_2 values if using the same Chua circuit. Furthermore, it would be an interesting study to determine what exactly causes the semi-chaotic regime to arise instead of the chaotic Lorenz attractor behavior in circuits similar to our manually constructed circuit, and to determine what the periodicity of the circuit is caused by.

Acknowledgements: Thank you to my partner, Adin Viera, and to the lab TAs, Joshua and Oorie.

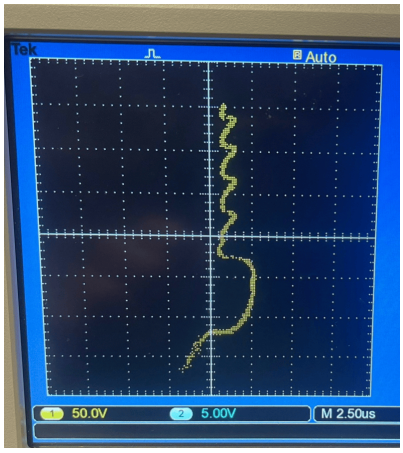

Figure 11: (a) 7 V, 20 kHz Square Wave

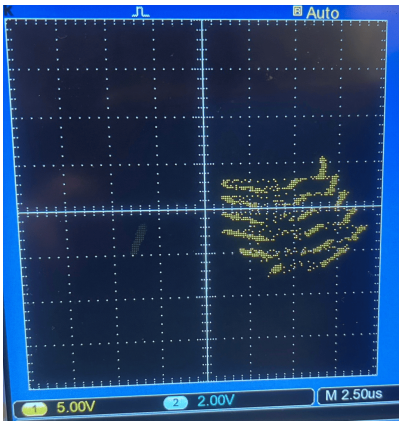

Figure 12: (b) 9 V, 2 kHz Square Wave

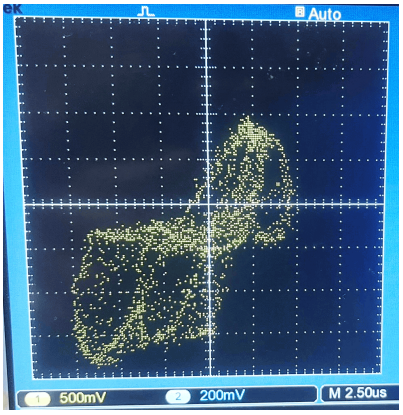

Figure 13: (c) 9 V, 200 kHz Triangle Wave

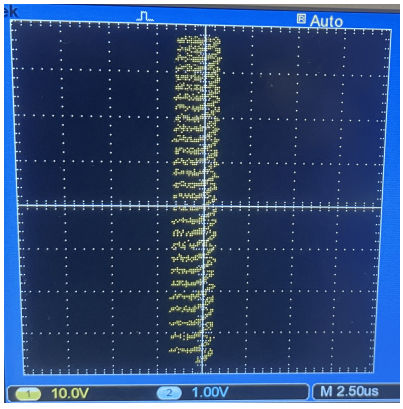

Figure 14: (d) 7 V, 20 kHz Sine Wave

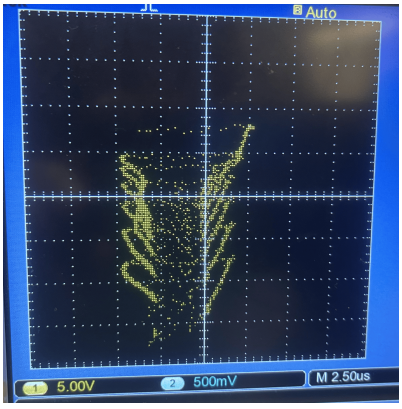

Figure 15: (e) 7 V, 30 kHz Sine Wave

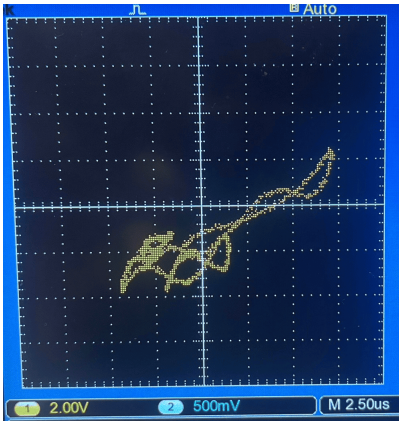

Figure 16: (f) 9 V, 2 MHz Triangle Wave

Figure 17: Different function generator waveforms passed into the manually-assembled iteration of the Chua circuit. The output shows interesting chaotic attractor-like behavior and unique shapes in phase space that are extremely sensitive to minor changes in waveform input.

References

[1] Valentin Sidersky et al. "Chua's Circuit for Experimenters Using Readily Available Parts from a Hobby Electronics Store". In: *Proceedings of the 122nd ASEE Annual Conference and Exposition*. Seattle, WA, June 2015. URL: https://web2.ph.utexas.edu/~phy353l/ChaoticDynamics/chua-s-circuit-for-chaos.pdf.

[2] Drew Baden. *An Introduction to Chaos*. 2020. URL: https://physics.umd.edu/hep/drew/numerical_integration/chaos.html.

[3] 2.04 : Bifurcations. LibreTexts. Accessed: 2025-11-23. 2025. URL: https://math.libretexts.org/Courses/Monroe_Community_College/MTH_225_Differential_Equations/02%3A_First_Order_Equations/2.04%3A_Bifurcations.

[4] Jarred Caldwell and Alex Vahidsafa. *Propagation of Error*. Online article, Chemistry LibreTexts. Accessed: 2025-11-24. 2023. URL: https://chem.libretexts.org/Bookshelves/Analytical_Chemistry/Supplemental_Modules_(Analytical_Chemistry)/Quantifying_Nature/Significant_Digits/Propagation_of_Error.

[5] Eric Chasnov. *11.02: Bifurcation Theory*. LibreTexts. 2025.

[6] LibreTexts Statistics Contributors. *2 : Kernel Density Estimation (KDE)*. LibreTexts. Accessed: 2025-11-23. 2025. URL: https://stats.libretexts.org/Bookshelves/Computing_and_Modeling/RTG%3A_Classification_Methods/2%3A_Kernel_Density_Estimation_(KDE).

[7] R. Delbourgo, W. Hart, and B. G. Kenny. "Dependence of universal constants upon multiplication period in nonlinear maps". In: *Phys. Rev. A* 31 (1 Jan. 1985), pp. 514–516. DOI: 10.1103/PhysRevA.31.514. URL: https://link.aps.org/doi/10.1103/PhysRevA.31.514.

[8] scikit-learn developers. *Density Locator — Kernel Density Estimation*. scikit-learn documentation. Accessed: 2025-11-23. 2025. URL: https://scikit-learn.org/stable/modules/density.html.

[9] N. Lorenz Edward. "Deterministic Nonperiodic Flow". In: *Journal of the Atmospheric Sciences* 20.2 (1963). Manuscript submitted 18 November 1962; revised 7 January 1963., pp. 130–141. DOI: 10.1175/1520-0469(1963)020<0130:DNF>2.0.CO;2. URL: https://cdanfort.w3.uvm.edu/research/lorenz-1963.pdf.

[10] Mitchell J. Feigenbaum. *Universality in Complex Discrete Dynamics*. Technical Report (LA-6816-PR). Report covers July 1975–September 1976. Theoretical Division, Los Alamos Scientific Laboratory, 1976. URL: https://chaosbook.org/extras/mjf/LA-6816-PR.pdf.

[11] Henry Greenside. *Orbit Diagram of the Logistic Map*. 2024. URL: https://webhome.phy.duke.edu/~hsg/513/images/logistic-map-orbit-diagram.html.

[12] Kristjan Haule. *Logistic Map and Lyapunov Exponent — Chaos in a Simple Nonlinear Map*. 2024. URL: https://www.physics.rutgers.edu/~haule/488/LogisticMap/Logistic%5C%20map.html.

[13] Mario Hieb. *Is the Electron Charge a Mathematical Constant?* viXra e-print archive: 1704.0365v1. 2017. URL: https://vixra.org/pdf/1704.0365v1.pdf.

[14] Tektronix Inc. *TBS1000 Series Digital Storage Oscilloscope – User Manual*. Accessed via Tektronix website. 2021. URL: https://www.tek.com/en/oscilloscope/tbs1000-digital-

storage-oscilloscope-manual/tbs1000-series-0.

[15] Texas Instruments Incorporated. *TL082,Wide Bandwidth Dual JFET Input Operational Amplifier Datasheet (Rev. O)*. Datasheet PDF. Accessed via internal path. 2013.

[16] Makoto Itoh, Ljupco Kocarev, and Kevin Eckert. "Chaos synchronization in Chua's Circuit". In: *Journal of Circuits, Systems and Computers* 03 (Nov. 2011). DOI: 10.1142/S0218126693000071.

[17] Hiroki Sayama. *9.03 Lyapunov Exponent*. LibreTexts. Accessed: 2025-11-23. 2025. URL: https://math.libretexts.org/Bookshelves/Scientific_Computing_Simulations_and_Modeling/Introduction_to_the_Modeling_and_Analysis_of_Complex_Systems_(Sayama)/09%3A_Chaos/9.03%3A_Lyapunov_Exponent.

[18] Andrei Vieru. "Bifurcations, Schwarzian derivatives and Feigenbaum constant revisited". In: *arXiv preprint arXiv:0802.3313* (2008). Submitted 22 Feb 2008; Revised 24 Jun 2008. URL: https://arxiv.org/pdf/0802.3313.

[19] Christos Vozikis, Konstantinos Kleidis, and Stavros Papaioannou. *The power spectrum indicator: A new, efficient method for the early detection of chaos*. 2018. arXiv: 1808.00223 [nlin.CD]. URL: https://arxiv.org/abs/1808.00223.

[20] Eric W. Weisstein. *Fast Fourier Transform*. From MathWorld–A Wolfram Resource. Accessed: 2025-11-23. 2000. URL: https://mathworld.wolfram.com/FastFourierTransform.html.